doi.org/10.52568/001439/JCSP/46.02.2024

Carbon Paste Electrode Modified with PMBP: A Sensitive Sensor for Electrochemical Detection of Acetaminophen

[1,2]Emi Norzehan Mohamad Mahbob, [1,3]Mohamad Syahrizal Ahmad*, [1,3]Illyas Md Isa**
[1,3]Norhayati Hashim, [4]Anwar Ul-Hamid, [1,3]Mohamad Idris Saidin and [5]Suyanta M. Si
[1]Nanotechnology Research Centre, Faculty of Science and Mathematics, Universiti Pendidikan Sultan Idris, 35900 Tanjong Malim, Perak Darul Ridzuan, Malaysia.
[2]Faculty of Applied Sciences, Universiti Teknologi MARA, Perak Branch, Tapah Campus, Tapah Road, 35400 Perak Darul Ridzuan, Malaysia.
[3]Department of Chemistry, Faculty of Science and Mathematics, Universiti Pendidikan Sultan Idris, 35900 Tanjong Malim, Perak Darul Ridzuan, Malaysia.
[4]Center for Engineering Research, Research Institute, King Fahd University of Petroleum & Minerals, Dhahran 31261, Saudi Arabia.
[5]Department of Chemistry Education, Faculty of Mathematics and Natural Science, Yogyakarta State University, Indonesia.
syahrizal@fsmt.upsi.edu.my*; illyas@fsmt.upsi.edu.my**

(Received on 03rd February 2023, accepted in revised form 23rd October 2023)

Summary: In this present work, a sensitive electrocatalytic modified electrode based on 1-phenyl-3-methyl-4-benzoyl-5-pyrazolone (PMBP)/multiwalled carbon nanotubes (MWCNT) modified carbon paste electrode (CPE) was successfully developed. Electrochemical impedance spectroscopy, square wave voltammetry, chronocoulometry and cyclic voltammetry were used in prompt to evaluate the PMBP/MWCNT/CPE electrochemical capacity in detecting acetaminophen (APAP) in 0.1 M PBS pH 6.4. Under optimized conditions, PMBP/MWCNT/CPE displayed a well-defined electrocatalytic activity towards APAP oxidation in the linear responses which range from 1 μM to 1 mM (R^2 = 0.991) with the LOD obtained at 0.245 μM while LOQ 0.816 μM. The presence of excess (10-fold and 25-fold) interferents such as sucrose, fructose, glucose, sodium chloride, sodium sulphate, potassium nitrate, lysine, potassium chloride and magnesium chloride as interferents was insignificant. The results presented in this study provide new perspectives on PMBP as a potential nanomaterial in the development of APAP sensors. As a conclusion, the PMBP/MWCNT/CPE revealed good stability, reproducibility, and repeatability, and was discovered to be relevant for usage in the pharmaceutical samples with satisfactory performance.

Keywords: Acetaminophen. Voltammetry. Multiwalled carbon nanotubes. Pyrazolone. Electrochemical impedance spectroscopy. Chronocoulometry.

Introduction

A revolution in voltammetry begun in the early 1960s after series of analytical methods were reported during those years [1]. Electrochemical sensors are often utilised as an analytical technique due to their great sensitivity as well as accuracy. The sensors are getting progressively exact and profoundly delicate when connected with nanotechnology [2]. Additionally, they are highly desirable due to the experimental simplicity, low cost, and amazing detectability when compared to the thermal, mass, and optical sensors [3]. Hence, to generate electrical currents which are proportionate to the analyte's concentration, the applied voltage serve as a driving force for electrocatalysis to occur [4]. However, without modification to the conventional electrodes surface, the response of this analyte is low. Therefore, several attempts of the electrode surfaces modifications have been made to enhance their voltammetric response due to increase electrocatalytic activities of the electrode. Because of these desired criteria, new modifier materials that display excellent electrochemical performance are being established continuously [5]. Numerous research done on acetaminophen (APAP) sensing have used carbon nanomaterials with multi-walled carbon nanotube (MWCNT) as an example because of the great potential possessed by these materials as electrode modifiers such as great electrical conductivity, mechanical stability and large surface area which aid in accelerating the electron transfer rate [6]. Still, those features will also depend on the materials available in the modifier.

*To whom all correspondence should be addressed.

The pain relief APAP, known as paracetamol, is an organic chemical that frequently used in pharmaceuticals [7]. APAP have endlessly been introduced into the aquatic environment from consumer use, disposal, manufacturing facilities, and hospital waste [8]. Harmful effects at low levels of APAP such as chronic and acute damages to aquatic organisms, cell proliferation inhibition in human cells as well as reproductive damages have been documented [9]. High transformation rate and non-stop induction of the pollutant into the environment, could trigger long-term damaging effects [10]. Therefore, analytical techniques which are sensitive for determining APAP, one of the electroactive molecule in different biological samples and environmental are required. Some researchers have developed different modified electrodes for the determination of APAP including CZTS/MoS_2/CNT [7], Gd_2ZnMnO_6/ZnO/Ionic liquid/CPE [11], CPE/NiZ/GO [12], CdO/MCPE [13], MWCNT/GO/Poly (Thr)/GCE [14], ND@Dy_2O_3-IL/CPE [15], and Stv-CPE [16]. In this work, carbon paste electrode (CPE) was chosen for the electrochemical sensor preparation because of unique properties including wide cathodic and anodic functions, comfortable surface renewability and low background current [17]. Significant reduction of potential overpotential and selective interaction between analyte and electrode are the main reasons for this improvement. Thus, cyclic voltammetry (CV) and square wave voltammetry (SWV) approaches have been reported for selective and sensitive APAP determination [5].

Fourteen decades ago, a German chemist, Ludwig Knorr successfully synthesized the first pyrazolone by mixing phenyl hydrazine and ethyl acetoacetate [18]. Today, pyrazolone-based ligands have become desirable compounds as they possess diverse functional medicinal properties including anti-inflammatory, antioxidant, anti-diabetic, analgesic, anti-proliferative, anti-microbial, anti-tumor, and many other biological activities [19-21]. Furthermore, the pyrazolone-based ligands are promptly becoming popular due to their usage in catalysis, in functional materials and as pigments for dyes as well as in sensors [22]. Acylpyrazolones for example have become the compound of interest as they play a key role in coordination chemistry. They have been applied in several areas, such as metal extraction agents [23]. The neutral acylpyrazolones exist in three different tautomeric forms which are 3-pyrazolone, 4-pyrazolone, and 5-pyrazolone [18]. The enol form OH in the acylpyrazolone present acidic properties which make this ligand suitable material for electrochemical analysis [24]. In previous research, an acylpyrazolone namely 1-phenyl-3-methyl-4-(2-furoyl)-5-pyrazolone (HPMαFP) has been employed for electrochemical detection of thyrosine [21], ofloxacin [24], xanthine [25], guanine [26], adenine and amino acid [27]. Another acylpyrazolone known as 1-phenyl-3-methyl-4-heptanoyl-pyrazalone-5 (HPMHP) has been used to determine the electrochemical behaviors of tin [23]. 1-phenyl-3-methyl-4-benzoyl-5-pyrazolone (PMBP) is also a type of acylpyrazolone and based on the literature survey done, it reveals that there was no attempt in employing PMBP through voltammetric activity to examine APAP. Yet this study intends to explore the electrochemical performance of PMBP in detecting the targeted bio-analyte.

Experiment

Materials

All reagents utilised in this experiment were analytical grade and utilised as received. Multiwalled carbon nanotubes (MWCNT) were bought from Timesnano, China. Acetaminophen, potassium chloride (KCl) and sodium hydroxide (NaOH) pellets were obtained from Sigma-Aldrich, the USA. Hydrochloric acid (HCl) was gained from Merck. Paracetamol tablets (0.5 g) were bought from a pharmacy in Tapah, Perak. Phosphate buffer solutions (PBS) with different values of pH were prepared by mixing up the stock solutions containing 0.1 M potassium dihydrogen phosphate (KH_2PO_4) and 0.1 M dipotassium hydrogen phosphate (K_2HPO_4) (Merck, Germany). Stock solutions (0.01 M) were freshly ready by dissolving the tablets in deionized water and kept at 4 °C prior to being used.

Instrumentation

The characteristics of PMBP were determined utilising a Fourier Transform Infrared (FTIR) model Cary 630 (Agilent, USA), an X-ray diffraction (XRD) instrument model Rigaku 600 (MniFlex, Japan), and a nuclear magnetic resonance (NMR) spectroscopy (NMR, JNM-ECX 500 JEOL, Japan) to get ^{1}H and ^{13}C NMR spectra. The XRD data were analyzed using X'Pert HighScore Plus software. Voltammetric analyses and electrochemical impedance spectroscopy (EIS) were executed employing a Potentiostat Series-G750 (USA) and a Galvanostat/Potentiostat model Ref 3000 (Gamry, USA), respectively. A standard of three electrode cells with a working electrode: PMBP or bare MWCNT paste electrodes; a counter electrode: a platinum wire; an Ag/AgCl electrode MF-2052 (Bioanalytical system, USA): a reference electrode, was used to measure the electrocatalytic activities. To determine the solution's pH, the Thermo Scientific Orion 2-Star Benchtop pH Meter (USA) was utilised. Finally, the real samples validation analysis was conducted by using high performance liquid chromatography (HPLC).

Synthesis of 1-phenyl-3-methyl-4-benzoyl-5-pyrazolone (PMBP)

The PMBP compound was developed utilising the benzoylation process based on previous work with slight modifications [28]. This method is based on direct benzoylation of pyrazolone with benzoyl chloride in the presence of sodium hydroxide. 7.5 g of 1-phenyl-3-methyl-5-pyrazolone (PMP) was weighed and put in a boiling flask. 45 ml of 1, 4-dioxane was then added to the PMP before it was gentle heated and stirred using a magnetic stirrer till it became fully dissoluted. The 3 M NaOH solution was added, and the mixture was stirred under vigorous stirring. 5 ml of benzoyl chloride was put into the mixture drop by drop and refluxed for 1 hour. The reaction mixture was then cooled to room temperature and put into 75 ml 3 M HCl. The solid phase produced was filtered off, then washed with methanol-water, and next dried on air. The synthesis process of PMBP is shown in Scheme-1.

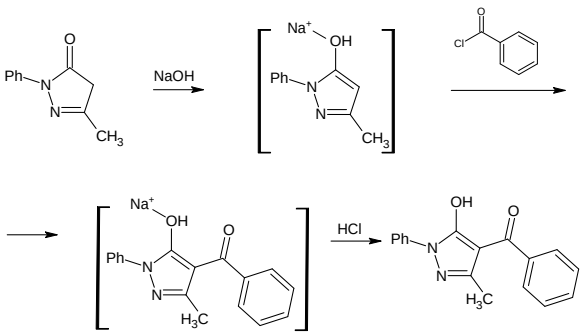

Scheme 1**:** Synthesis process of 1-phenyl-3-methyl-4-benzoyl-5-pyrazolone (PMBP).

Electrode fabrication and modification

For the electrode fabrication, a 100 mg of MWCNTs with different amount of PMBP (5, 10, and 15 mg, respectively) were mixed by hand mixing the mixture with three drops of paraffin oil and ground carefully using mortar and pestle until the paste was homogenized. Next, the produced carbon paste was loaded firmly into Teflon tube (2 mm in diameter and 5 cm long). One of the tube's ends was inserted with copper wire to create the electrical contact, whilst the other tube's end was polished with a soft paper prior to being used. The bare MWCNT electrode was made by utilising the same procedure with no addition of PMBP for comparison purpose.

Results and Discussion

Characterization of PMBP

The characterization by infrared spectroscopy (Fig. 1) was recorded in the range of 4000-400 cm^{-1}. The spectrum showed a vibration weak band on $\bar{\upsilon}$ = 3052 cm^{-1} that was dedicated to C-H aromatic stretching. The sharp and strong band of $\bar{\upsilon}$ = 1598 cm^{-1} and $\bar{\upsilon}$ = 1554 cm^{1} were related to the C = C aromatic vibration and the vibration of C = O, respectively. The band attributed to the C-N of the pyrazolone ring appeared at $\bar{\upsilon}$ = 1496 cm^{-1} and reappeared at $\bar{\upsilon}$ = 1190 cm^{-1}. The C-H vibration band of the methyl group (-CH_3) appeared at $\bar{\upsilon}$ = 1452 cm^{-1} and the vibration band O-H occurred at $\bar{\upsilon}$ = 1352 cm^{1} and $\bar{\upsilon}$ = 1142 cm^{-1}, whereas the pyrazolone framework's peak appeared at $\bar{\upsilon}$ = 946 cm^{-1}.

The spectrum of ^{1}H NMR (Fig. 2a) exhibited a singlet signal at δ_H = 2.11 ppm which was assigned to the -CH= group. The triplet signal at δ_H = 7.29 - 7.33 ppm indicated one proton at C_4 of benzene while the triplet signal at δ_H = 7.46 - 7.48 ppm was ascribed to the two protons on C_3 and C_5 atoms of the benzene ring. The pyrazolone skeleton appeared at δ_H = 7.49 - 7.53 ppm. The ^{13}C NMR (Fig. 2b) analysis of the C carbonyl signals at C_4 and C_5 at δ_C = 192.19 ppm and 148.08 ppm. The signal at δ_C = 15.95 ppm was due to C_1 from methyl. The signals at δ_C = 161.50 ppm and 103.68 ppm were assigned to the C_2 and C_3 of the pyrane ring, the signals at δ_C = 127.98 - 128.89 ppm were related to the C_1 - C_6 of benzene ring and the signals that appeared at δ_C = 129.25 ppm - 137.70 ppm belong to the C_1 - C_6 from the pyrazolone framework. The results were compared with that obtained by [29]. Therefore, it can be concluded that the PMBP synthesized was pure and these characterizations were in agreement with the PMBP.

SEM was used to assess the morphology of PMBP and fabricated PMBP/MWCNT. Fig. 3a shows typical image of MWCNTs as a network structure which is entangled and dense. Meanwhile, the SEM image of PMBP displays irregular shaped block-like structures with rough morphology as depicted in the Fig. 3b. This roughness can be attributed to the presence of cavities on its surface [30]. The PMBP was scattered uniformly on the wall of MWCNT which showed that MWCNT was successfully modified by PMBP (Fig. 3c), which might increase the area of the modified electrode surface. Thus, this promoted the peak currents of APAP oxidation.

To identify the phases and crystal structures of the fabricated PMBP/MWCNT, the X-ray diffraction method was employed. Fig. 4 represents the diffractogram of PMBP with the prominent diffraction peaks of the synthesized PMBP which appeared at average 2θ of 6.59°, 17.78°, 18.64°, 19.88°, 21.77°, 24.86°, 25.71°, 28.02°, and 32.14°. A broad peak at 2θ = 19.88° was attributed to its amorphous character.

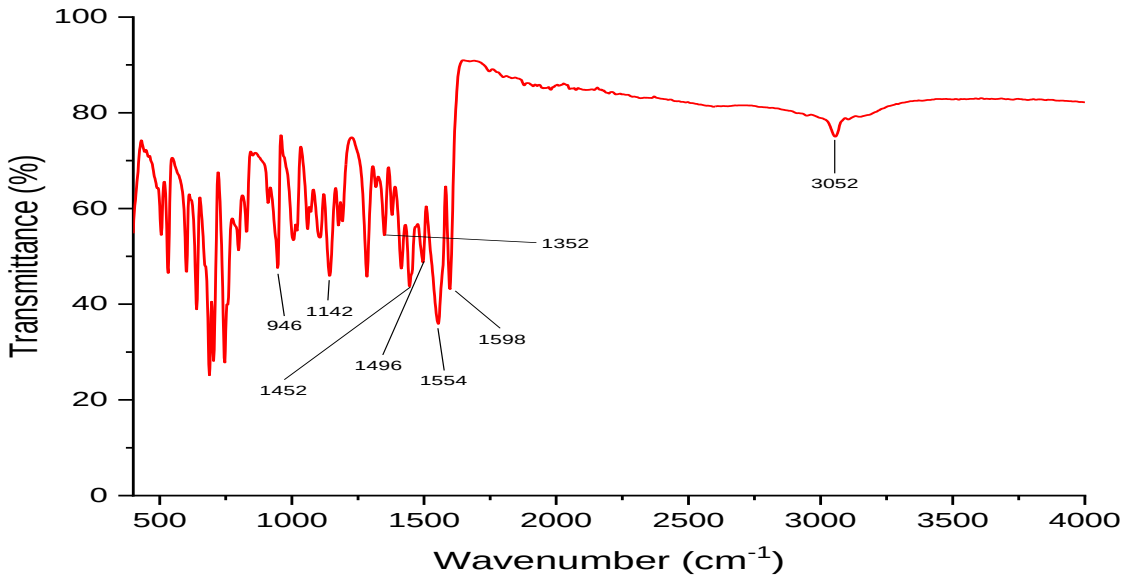

Fig. 1: FTIR spectrum of the PMBP.

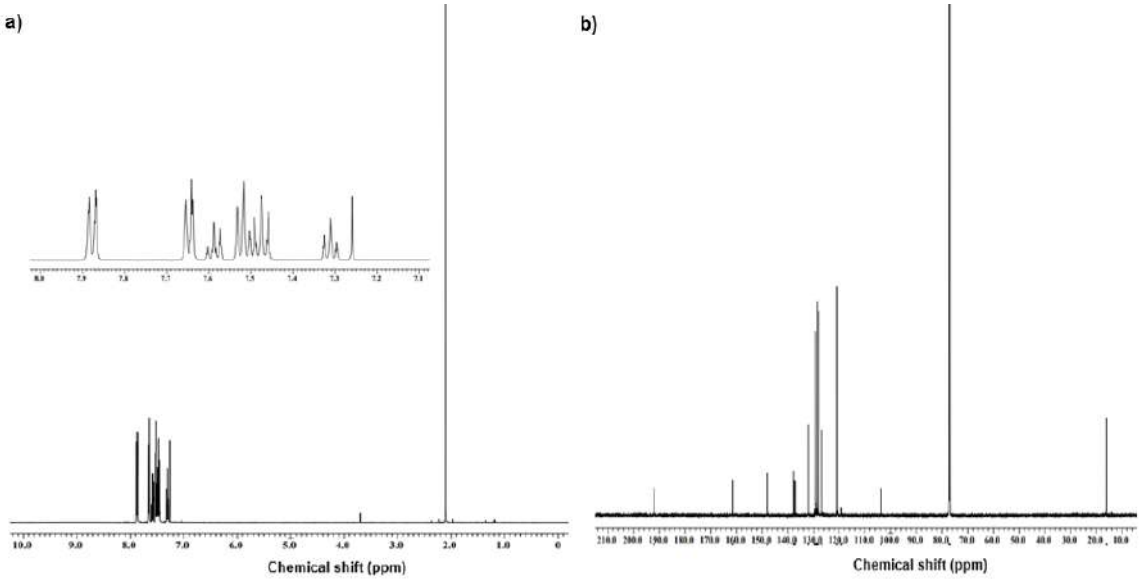

Fig. 2: a) ^{1}H, and b) ^{13}C NMR spectra of the PMBP.

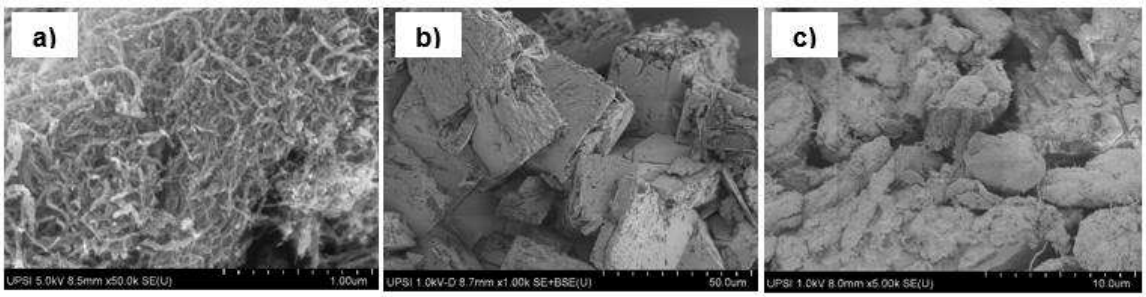

Fig. 3: a) The SEM image of a MWCNTs, b) PMBP, and c) PMBP/MWCNT.

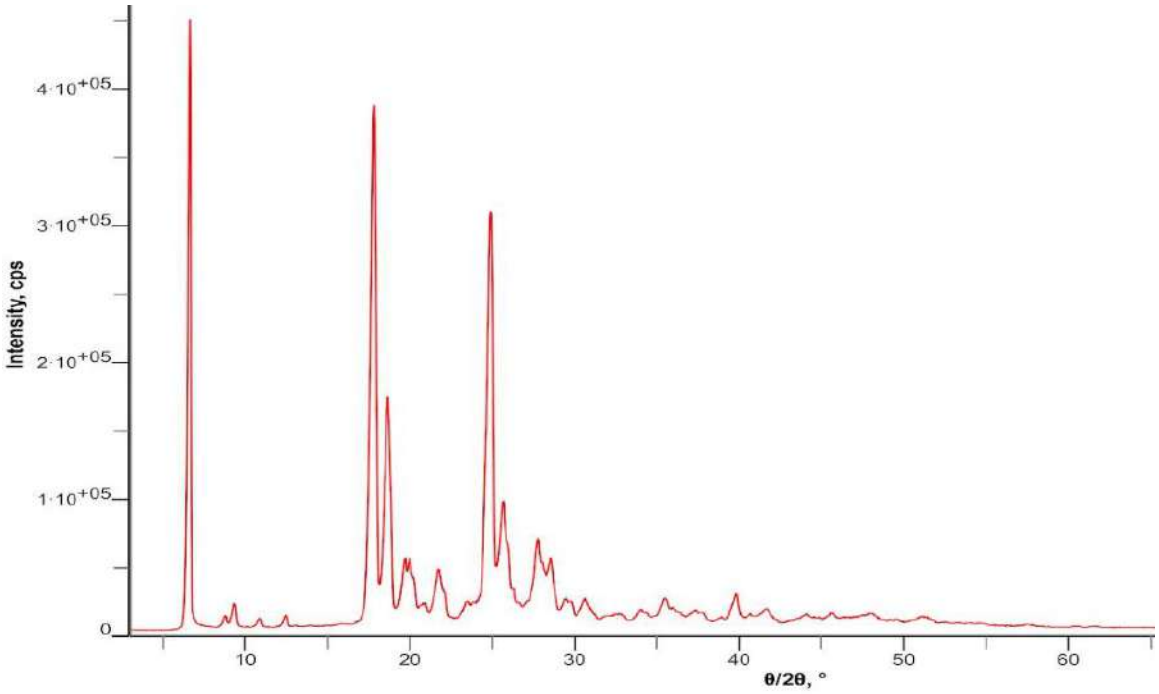

Fig. 4: Diffractogram of PMBP.

In addition, the peaks broadness can be utilised to acquire the PMBP crystallite size by employing the Debye–Scherrer formula in Eq. 1 as follows:

$$D = \frac{K\lambda}{\beta cos\theta} \quad (1)$$

where K is the Scherrer's coefficients (0.90), λ = the X–ray wavelength, typically 0.1541 nm, D = the average crystallite size of the prepared particles, θ is Bragg's angle and β is the full width at half maximum (FWHM) in radians. The produced PMBP have an average calculated crystallite size of 15.38 nm.

Electrochemical performance of the PMBP/ MWCNT/CPE

The modified electrode, PMBP/MWCNT/CPE electrochemical activity has been explored via electrochemical impedance spectroscopy (EIS), and cyclic voltammetry (CV) utilising standard redox system of 4 x 10^{-3} M $K_4[Fe(CN)_6]$ containing 100 mM KCl as a reference. The comparative voltammograms of the electrodes, bare MWCNT/CPE and PMBP/MWCNT/CPE are shown in Fig. 5 in which reversible redox peaks are seen. In a bare MWCNT alone, redox peak currents appeared at cathodic peak current (I_{pc}), 3.267 µA, and anodic peak current (I_{pa}), 7.314 µA, respectively. Meanwhile, the oxidoreduction peak current of PMBP/MWCNT paste electrode was enhanced to I_{pa} = 7.747 µA and I_{pc} = 3.899 µA. In addition, PMBP/MWCNT paste electrode peak-to-peak separation (ΔE_p) was found to be decreased one times lower with respect to bare MWCNT. The displayed results showed that the integration of PMBP and MWCNT paste electrode contributed improvisation of the electrode electrochemical response in the matter of conductivity, and electron-transfer rate [31].

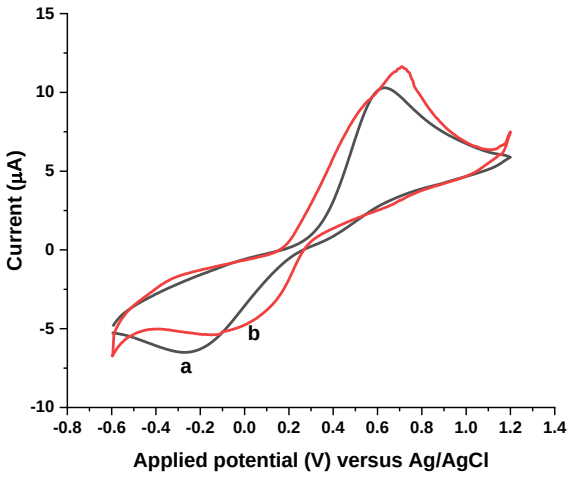

Fig. 5: Cyclic voltammograms of (a) bare MWCNT/CPE, and (b) PMBP/MWCNT/CPE for 4 mM $K_4[Fe(CN)_6]$ in 100 mM KCl, at 100 mV/s as scan rate.

The electrochemical properties and sensitivity of modified electrodes in 0.1 mM APAP using 100 mM phosphate buffer (pH 6.4) as a supporting electrolyte was

also investigated using CV. Potential range employed for this study was -0.3 V to 1.2 V. CV plots for 0.1 mM APAP of bare MWCNT and PMBP/MWCNT electrodes are presented in Fig. 6. In the CV, a bare MWCNT displayed a weak electrocatalytic oxidation current for APAP. However, the excellent and well-defined peak with maximum current and resolution was observed at PMBP/MWCNT, which indicates that the APAP electrochemical oxidation is more viable at the modified electrode. The APAP response current observed at PMBP/MWCNT is slightly larger than that on bare MWCNT itself. The outcomes are aligned with the response of the modified electrode towards $K_4[Fe(CN)_6]$ where it is mainly attributed to the integration effects of PMBP and MWCNT. Furthermore, it also can be found from the Fig. 6 that APAP displays quasi-reversible wave with oxidation peak on further scan and small reduction peak on the other side scan [32].

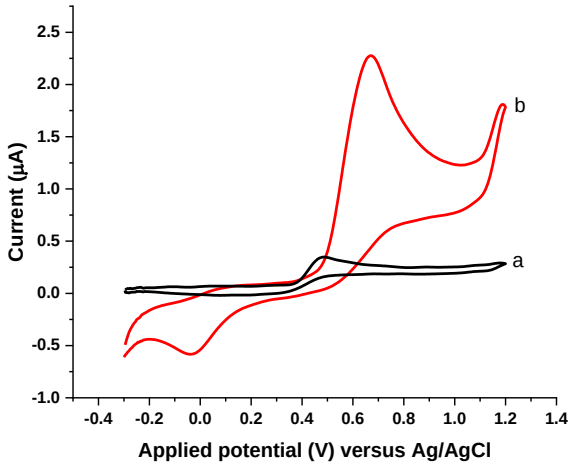

Fig. 6: CV of 100 μM APAP at the (**a**) bare MWCNT/CPE, and (**b**) PMBP/MWCNT/CPE in 100 mM PBS at 100 mV/s as scan rate.

EIS was used to investigate the electrode/electrolyte surface nature in which the transfer of electron process across the electrolyte/electrode interface of the modified sensors [33] and further validate the CV results [34]. The recorded impedance spectra of the bare MWCNT and PMBP/MWCNT in 0.1 M KCl with 4 mM $K_4[Fe(CN)_6]$ are shown using Nyquist plots (Fig. 7). Two parts in the plot representing linear portion at lower frequency and semicircle at higher frequency. The semicircle diameter presenting the electron transfer resistance (R_{ct}) at the interface of working electrode-electrolyte. The smaller arc radius of the EIS Nyquist plot represents the lower electron transfer resistance [35].

The biggest semicircle diameter possessed by the bare MWCNT/CPE compared to the PMBP/MWCNT/CPE, describing a slow interfacial electron transfer process. In contrast, the smaller semicircle diameter showed by PMBP/MWCNT/CPE justifying the presence of PMBP enhances the electron transfer process and reduces the impedance of the electrode. Furthermore, integration of the PMBP in the electrode raises the CPE's conductivity, hence decreases the resistance of electron transfer. The R_{ct} values are as follows: bare MWCNT (38.82 kΩ) > PMBP/MWCNT (7.87 kΩ). The results validate that the presence of PMBP assists electron transfer process. The impedance data was fitted to an equivalent circuit as shown in Fig. 7 (inset).

To determine the redox pair kinetic facility, the electrodes' electron transfer apparent rate constant, k_{app} must be calculated employing the gained R_{ct} value [36] and be fitted in the following equation (Eq. 2):

$$k_{app} = RT/n^2F^2AR_{ct}C \qquad (2)$$

where A is the microscopic area of the electrodes, n is the number of transferred electrons, while R, T, and F have their usual meanings. Therefore, the value of electron transfer apparent rate constant of the PMBP/MWCNT/CPE, derived from the Eq. 1 is 2.69 x 10^{-4} cm s^{-1} which is 4.93 times higher than the bare MWCNT (5.46 x 10^{-5} cm s^{-1}) demonstrating enhancement of charge transfer reaction kinetics [37]. Scheme 2 shows the APAP electro-oxidation process involving two protons and two electrons, and oxidation of the APAP on the modified surface of electrode during the electrochemical sensing.

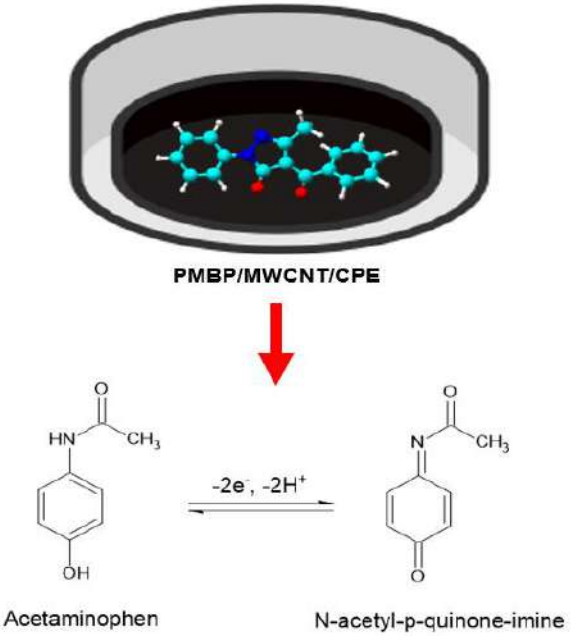

Scheme 2: Proposed reaction mechanism for APAP at PMBP/MWCNT/CPE.

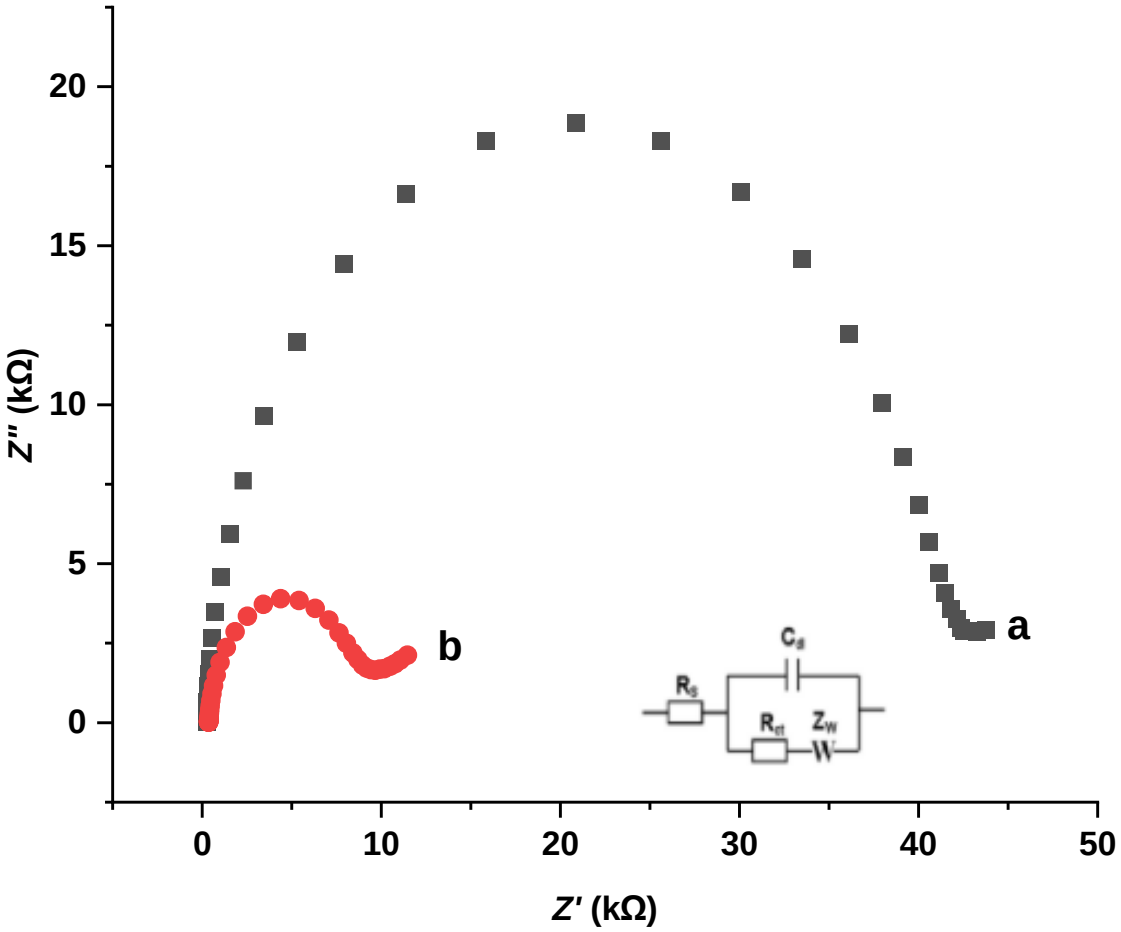

Fig. 7: The impedance spectra recorded for 4 mM $K_4[Fe(CN)_6]$ in 0.1 M KCl for (a) bare MWCNT, and (b) PMBP/MWCNT paste electrode with the Randles equivalent electrical circuit used for data fitting.

Optimization of the parameters for voltammetric analysis

The variation in the amount of modifier, as well as pulse size, step size and frequency of the SWV system affected the curve of the output voltammograms of the investigated analytes at PMBP/MWCNT. As well, the pH and scan rate of the supporting electrolyte influenced the electrocatalytic response at the PMBP/MWCNT.

Amount of modifier

This study has employed SWV to examine the electrocatalytic activity of different modifier contents (% w/w) between MWCNT and PMBP in 1 x 10^{-4} M APAP. As depicted in Fig. 8, it was found that by adding gradually the amount of modifier from 5 to 15 mg, the current responses were intensified with component ratios of PMBP in MWCNT paste electrode. This indicate that the addition of PMBP into the MWCNT has altered the electrode surface physicochemical properties preceding to the increment of its conductivity [38]. Hence, the modified MWCNT paste electrode with 15 mg of PMBP has been implemented for further experiments.

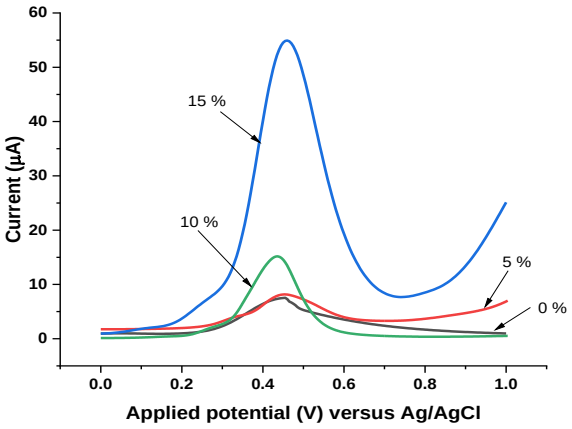

Fig. 8: Voltammograms of different percentages of PMBP on the 0.1 mM APAP's peak currents in 0.1 M PBS (pH 6.4).

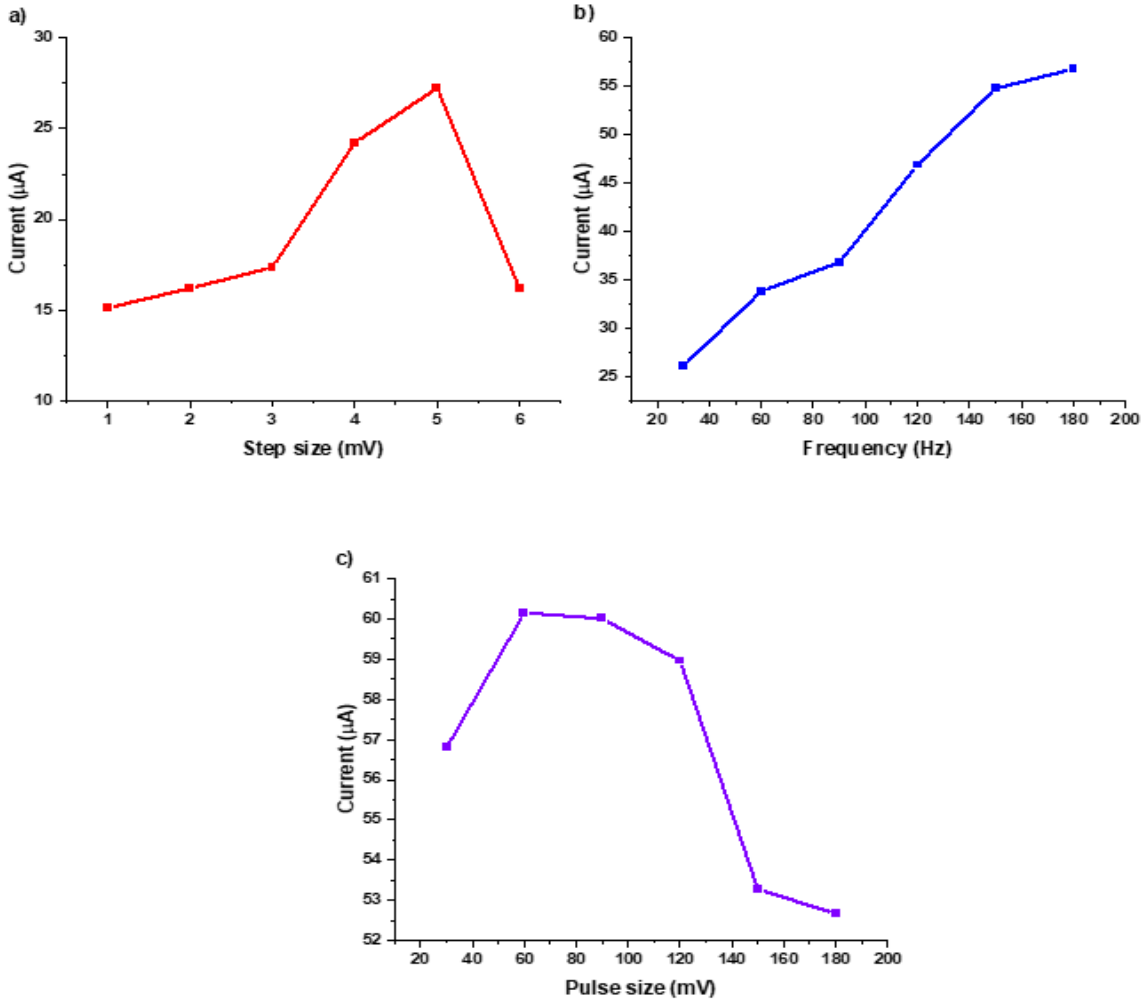

Fig. 9: Effects of the SWV parameters (**a**) step size, (**b**) frequency, and (**c**) pulse size on current response in solution of 0.1 mM APAP.

Effect of SWV parameters

Fig. 9a shows that the step size value of 5 mV was the optimum value for the APAP detection, setting step size at higher value did not lead to anymore increment in peak current response. The frequency values over the range of 30–180 Hz were evaluated through the study. Fig. 9b shows that APAP oxidation peak's height rises remarkably with higher frequencies, reaching its optimum at 180 Hz. As shown in Fig. 9c, the effect of pulse size has been investigated over the range of 30 to 180 mV. With the increment amount of pulse size, the peak heights recorded had displayed a significant increase in intensity up to 60 mV, then the peaks began to decline. Thus, the ideal SWV conditions (step size: 5 mV; pulse size: 60 mV; frequency: 180 Hz) were applied for all subsequent measurements due to better sensitivity and resolution.

Effect of scan rate

The dependency of the oxidoreduction peak potentials and peak currents towards the scan rate was examined to identify the performance of the sensing electrode's ability in transferring the charge by determining the type of mass transport involved [39]. CV was ran using 1 mM APAP in 0.1 M PBS at pH 6.4. The impact of scan rate on peak current and peak potential (E_p) is described in Fig. 10. It can be seen that the anodic peak potential (E_{pa}) is moved to positive potential meanwhile the cathodic peak potential (E_{pc}) to the negative value, respectively. This could be due to changes in the electrocatalytic activity and kinetic effect of PMBP/MWCNT/CPE surface on the redox reaction of APAP.

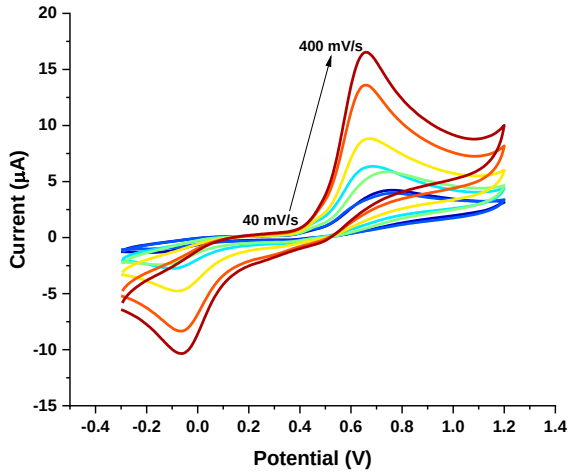

Fig. 10: Cyclic voltammograms of PMBP/MWCNT/CPE with 1 mM APAP at different scan rates (40 mV/s to 400 mV/s).

Moreover, it was also noticed that the oxidoreduction peak currents raised with the increment of scan rate over the range of 40 mV/s to 400 mV/s. Fig. 11 displays that the redox peak currents were proportionate to the scan rates. The fitted regression equations is stated as follows (Eq. 3, Eq. 4):

$$I_{\mathrm{pa}} = 0.0297v + 1.3068\ (R^2 = 0.9933) \quad (3)$$

$$I_{\mathrm{pc}} = -0.0156v + 0.2784\ (R^2 = 0.9923) \quad (4)$$

The linear correlation of the peak currents (I_{pc} and I_{pa}) with the scan rate (v) showed that the reaction occurred at PMBP/MWCNT is a surface-controlled process [40].

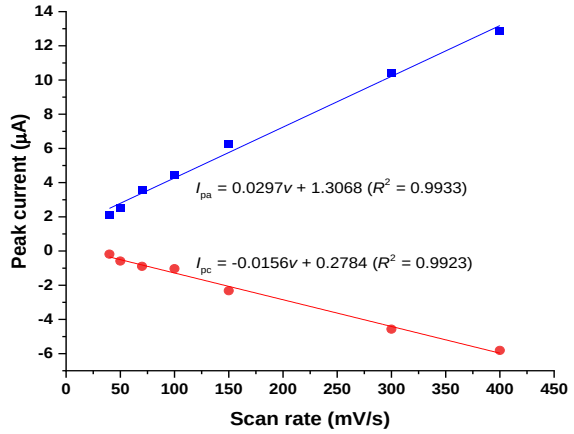

Fig. 11: The correlation between the redox peak currents of APAP and the scan rates.

Fig. 12 displays the plot of square root of different scan rates against the peak currents which displays a linear relationship between the two parameters, suggesting a process between scan rates and currents was a diffusion control principle. The linear regression equation (Eq. 5) tabulated from the oxidation peak currents is as follows:

$$I_{\mathrm{pa}} = 0.7869v^{1/2} - 3.1269\ (R^2 = 0.997) \quad (5)$$

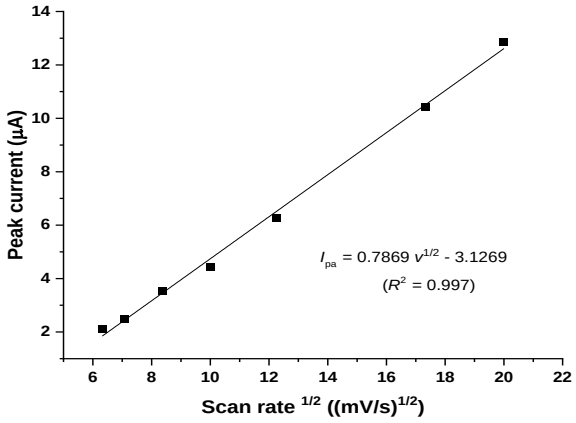

Fig. 12: The peak current against the square root of scan rate's plot.

In further, as displayed in the log anodic peak current against log scan rate's plot (Fig. 13), the peak current response also enhanced linearly with the scan rate with the linear regression equation (Eq. 6):

$$\log I_{\mathrm{pa}} = 0.7835 \log v - 0.9205\ (R^2 = 0.9979) \quad (6)$$

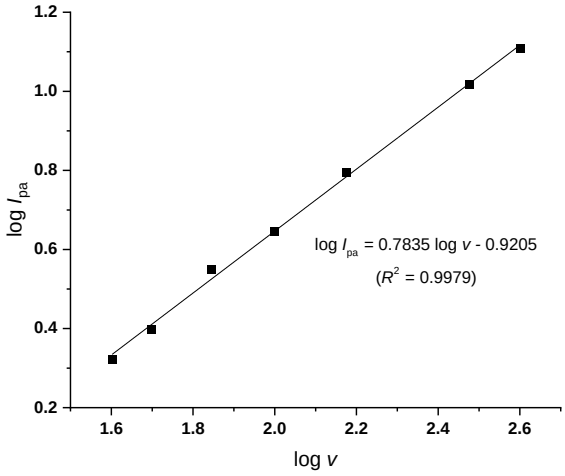

Fig. 13: The log peak current versus the log of scan rate's plot.

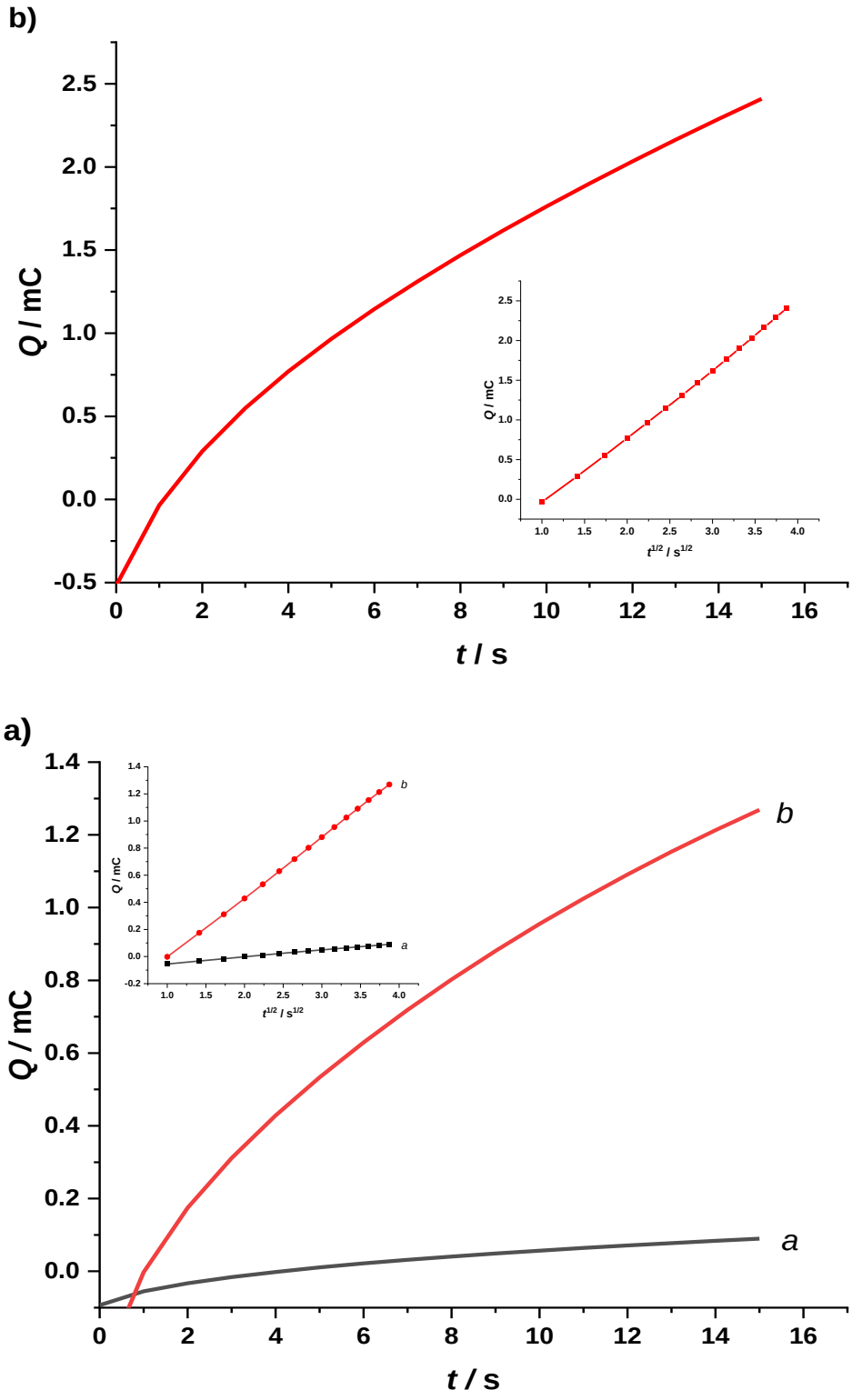

Fig. 14: (a) The chronocoulograms of (a) MWCNT/CPE, and (b) PMBP/MWCNT/CPE in 4 x 10^{-3} M $K_4[Fe(CN)_6]$, (b) the chronocoulograms of PMBP/MWCNT paste electrode in 100µM APAP (inset: plot of Q versus $t^{1/2}$).

From the equation, value of the slope was calculated to be 0.7835. The values of slope of log (I_{pa}) versus (log v) between 0.5 and 1.0 suggest the process that occurred at the sensor surface was a mixed diffusion-adsorption processes [39].

Chronocoulometry study

To compare the adsorption behavior of PMBP/MWCNT and bare MWCNT, this work utilised the chronocoulometry. The electrodes surface coverage has been calculated using the Anson's equation (Eq. 7):

$$Q(t) = \frac{2nFAD^{\frac{1}{2}}Ct^{\frac{1}{2}}}{\pi^{\frac{1}{2}}} + Q_{ads} \quad (7)$$

where electron surface area, charge, number of electrons transferred, diffusion coefficient, bulk concentration, Faraday constant and time are represented by A, Q, n, D, C, F and t, respectively [41]. By utilising the slope of Q versus $t^{1/2}$ (Fig. 14), the A value for the PMBP/MWCNT and bare MWCNT electrodes were found to be 0.583 and 0.066 cm^2, correspondingly. About 10-fold of increment was observed after the addition of the modifier PMBP, hence showing that an enhancement of current response of the modified electrode towards $K_4[Fe(CN)_6]$.

The value of Q_{ads} of APAP has also been identified using the intercept of the Q versus $t^{1/2}$ plot and determined to be 9.27 x 10^{-4} C. As a result, D was determined to be 4.52 x 10^{-3} cm^2s^{-1}. In addition, the adsorption capacity (Γ) of PMBP/MWCNT electrode was calculated using following relationship (Eq. 8):

$$Q_{ads} = nFA\Gamma \quad (8)$$

The calculated result showed that the surface coverage value was afforded as 8.24 x 10^{-9} mol cm^{-2}, thus displaying a good capacity of adsorption for APAP.

Effect of pH on the electrode performance

The supporting electrolyte pH is a significant factor that controls the electrochemical oxidoreduction that occurs at the electrode's surface. In this research, the pH's effect on the response of APAP (0.1 mM) was evaluated using square wave voltammetry technique over the pH range of 6.0-8.4 employing phosphate buffer solution (Fig. 15).

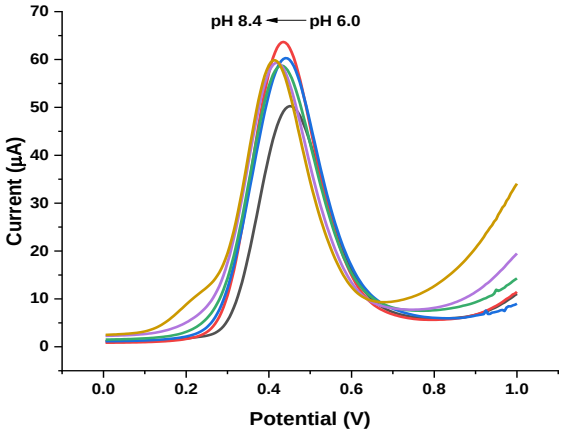

Fig. 15: pH's effects on peak currents (a = 60 mV, ΔES = 5 mV, f = 180 Hz).

When the value of pH changes from 6.0 to 6.4, the acetaminophen oxidation peak current increase in intensity, and when the pH elevated than 6.4, the acetaminophen oxidation peak current reduced. The reduction of the anodic peak current could be caused by the deprotonation in the oxidation process that favours a higher pH [42]. Acidic electrolytic solution encourages the migration of electron and in further acetaminophen oxidation [39]. Therefore, the PBS at pH 6.4 has been identified to be the ideal experimental parameter for the electrochemical detection method of the next experiment.

In addition, the correlation between peak potentials (E_p) and pH level is shown in Fig. 16. The linear regression equation (Eq. 9) of the correlation between the parameters is as follows:

$$E_p\ (mV) = -13.229\ \text{pH} + 526.74\ (R^2 = 0.9937) \quad (9)$$

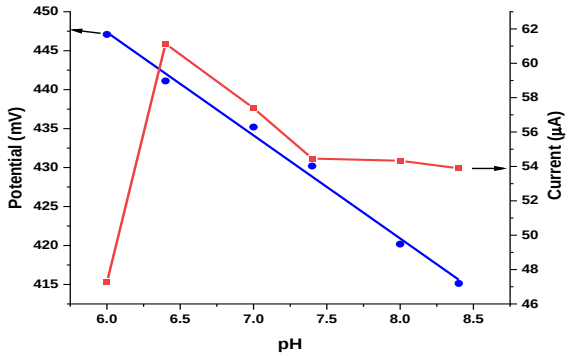

Fig. 16: Oxidation potential (E) and oxidation peak current (I) versus pH plot of 100 mM PBS containing 100 M APAP at PMBP/MWCNT paste electrode.

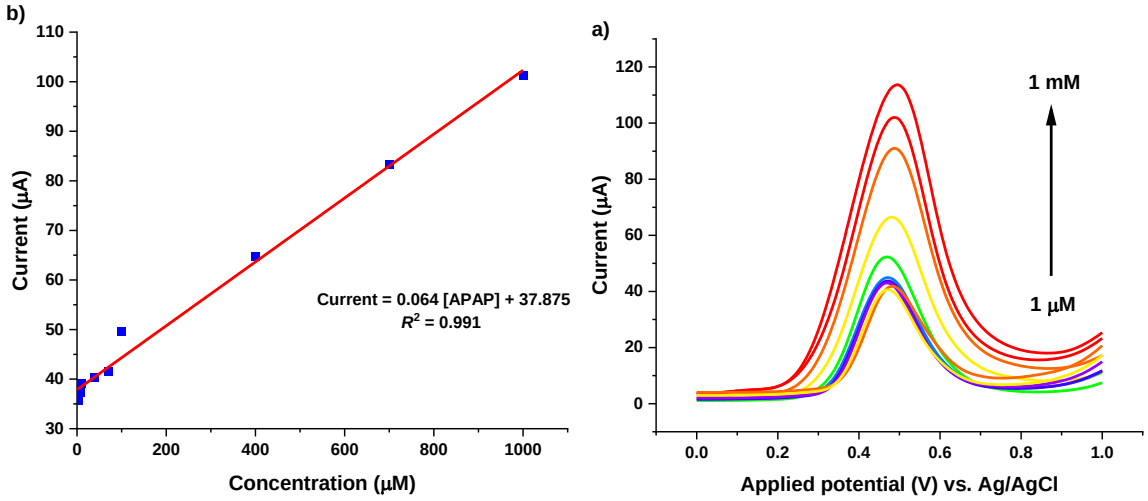

Fig. 17: (a) Square wave voltammograms and (b) corresponding calibration plot of 1 μM - 1 mM APAP in 100 mM PBS (pH 6.4) at PMBP/MWCNT/CPE.

Table-1: The difference of the modified sensor in the electrocatalytic activity of APAP.

Sensor	Method	Range (M)	LOD (M)	Ref.
ZLH-LP/MWCNT/CPE	SWV	7.00×10^{-7} - 1.00×10^{-4}	8.30×10^{-8}	[36]
SWCNT/Ni/GCE	CV	5.00×10^{-5} -5.00×10^{-4}	1.17×10^{-7}	[39]
P4VP/MWCNT GCE	DPV	2.00×10^{-8} - 4.50×10^{-4}	1.69×10^{-9}	[40]
Pt/NGr/GCE	SWV	5.00×10^{-8} -9.00×10^{-5}	8.00×10^{-9}	[44]
fCNTs/ZnO/fCNTs/GCE	SWASV	2.00×10^{-7} - 6.00×10^{-12}	5.06×10^{-5}	[45]
GCPE/RGO	SWV	4.00×10^{-6} - 2.20×10^{-5}	3.07×10^{-7}	[47]
Pt/OMC-GCE	DPV	7.00×10^{-8} -3.70×10^{-7} 3.70×10^{-7} -3.38×10^{-5}	1.50×10^{-8}	[48]
NiFe-CPE	DPV	6.00×10^{-7} -8.50×10^{-6}	8.00×10^{-8}	[49]
MWCNT-βCD/GCE	DPV	5.00×10^{-8} - 1.00×10^{-6} 1.00×10^{-6} - 3.00×10^{-4}	1.15×10^{-8}	[50]
PMBP/MWCNT/CPE	SWV	1.00×10^{-6} - 1.00×10^{-3}	2.45×10^{-7}	This work

The outcomes demonstrated that the peak potential changes negatively with the pH increment, which shows that the H^+ involves directly in the electrochemical process [43].

APAP concentration effect

The effect of different APAP concentrations in 100 mM PBS electrolyte solution with applied potentials of 0 to 1 V, step size 5 mV, frequency 180 Hz, pulse size 60 mV, and 100 mV/s as the scan rate, was explored at the PMBP/MWCNT. The method of SWV is desirable compared to CV because of the resolution, lower limit of detection (LOD), and sensitivity [44]. Series of excellent peaks were gained from the voltammetric responses to the addition of acetaminophen in the range of 1 to 1000 μM.

Fig. 17a exhibits the peak current increase in intensity by the increment of APAP concentration while Fig. 17b displays clearly that the electrocatalytic peak current of APAP oxidation was linearly proportionate to the APAP concentrations over the range of 1 μM to 1000 μM with the linear regression equation I (μA) = 0.064[APAP] (M) + 37.875 and the correlation coefficient (R^2) of 0.991.

The LOD and LOQ of targeted analytes can be evaluated from their IUPAC standard definitions as in Eq. 10 and Eq. 11:

$$LOD = 3\sigma / m \quad (10)$$

$$LOQ = 10\sigma / m \quad (11)$$

where m = the slope of calibration (concentrations versus current) plot and σ = the standard deviation of n times replicate of blank voltammograms recorded at the electrode surface in electrolyte solution only [45-46]. The LOD for this work was determined to be 2.45×10^{-7} M while LOQ, 8.16×10^{-7} M. The acquired data were compared with data reported by previous related work that used other modified sensors as listed in Table-1.

Interference study

The interference study in assessing the electrode response is crucial to discover the versatility and selectivity of the modified sensor, as well as to

design or prepare the sample, in order to minimise their disturbances in the analyses [51]. The anti-interference ability of the modified sensor is examined by adding up interferers to a 100 µM APAP in 0.1 M PBS. The effects of various inorganic and organic interfering substances were investigated on the oxidation signals of APAP (Fig. 18). 10-folds and 25-folds of concentrations of sucrose, fructose, glucose, sodium sulphate, sodium chloride, potassium nitrate, and lysine did not significantly affect the APAP current responses, and relative errors were found to be less than ± 10%. The results show that modified sensor displays a high selectivity for the APAP detection [52].

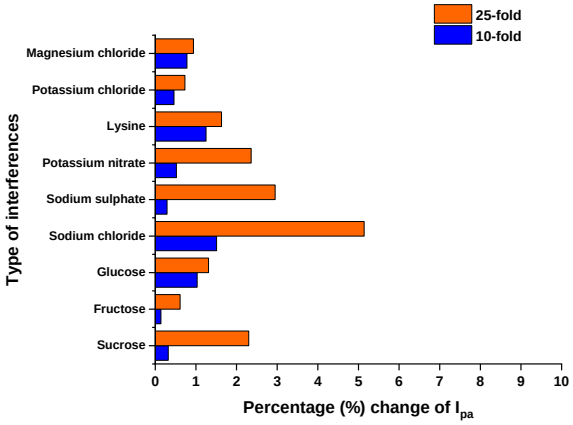

Fig. 18: Interference analysis of 0.1 mM APAP at PMBP/MWCNT/CPE.

Stability, reproducibility, and repeatability of the PMBP/MWCNT

Stability, repeatability, and reproducibility are crucial attributes in determining the modified electrode performance. All stated criteria were evaluated by monitoring the responses of the PMBP/MWCNT/CPE towards 0.1 mM APAP in 0.1 M PBS (pH 6.4). Four identically produced modified sensors were the subjects in the reproducibility test, and the relative standard deviation (RSD) was calculated to be 2.09 % (Fig. 19a). In addition, the repeatability was found to be 4.91 % when the RSD was calculated involving ten consecutive measurements with the same modified electrode (Fig. 19b). These results indicate that the PMBP/MWCNT/CPE was stable with good consistency displayed by the electrodes; hence they could be used for APAP detection.

The modified sensors' stability has been discovered through observing the current response to APAP determination after 14 days of execution. The produced current was seen to sustain around 90% of its initial response after 14 days of storage, indicating that the PMBP/MWCNT/CPE possess high stability.

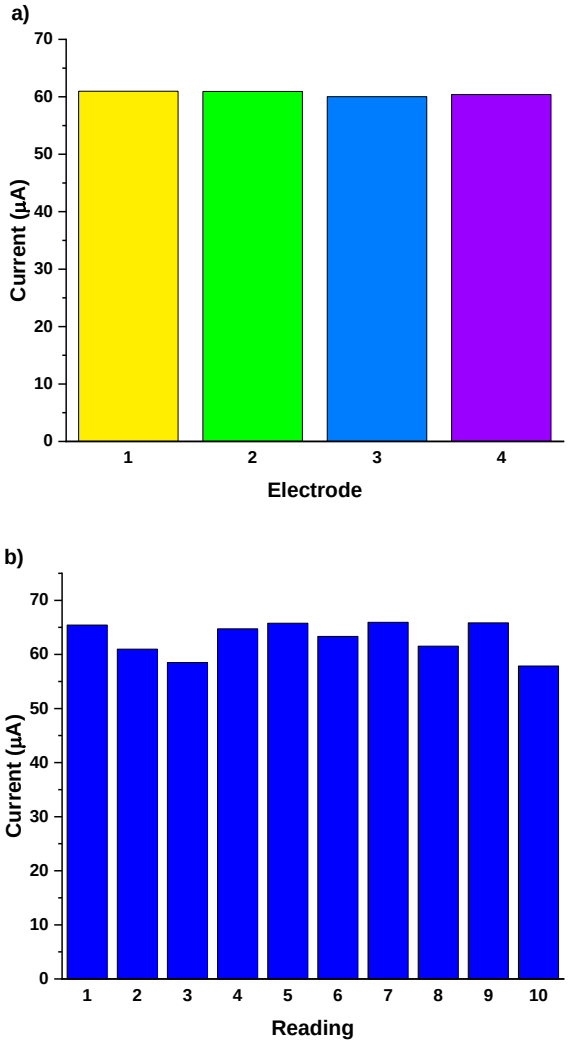

Fig. 19: (a) Reproducibility and (b) repeatability of PMBP/MWCNT/CPE.

Analytical application

To justify the significance of the suggested techniques and modified sensor for the APAP detection, by using the standard addition method, the pharmaceutical tablet containing APAP was investigated via SWV at PMBP/MWCNT/CPE. The findings were tabulated in Table 2. Good restoration of APAP was observed in the range of 91.61% to 107.60%: this further show the efficacy and reliability of this method. An independent *t*-test was made at a confident level of 95 % to investigate the correlation between the data gained from HPLC and SWV methods. Since *p*-value is greater than the significance level $p > .05$, the null hypothesis (H_0) failed to be

rejected, indicating that there is no significant difference between the results gained from HPLC and SWV methods.

Table-2: Quantification of APAP in commercially paracetamol tablet sample at PMBP/MWCNT/CPE.

Sample	Added (M)	Found (M)	Recovery (%)
Commercial paracetamol tablet	**25**	**22.90**	**91.61**
	35	**37.66**	**107.60**
	45	**43.62**	**96.94**

Conclusion

This work reported the fabrication of simple and sensitive electrochemical sensor PMBP/MWCNT/CPE in sensing APAP. Various compositions of PMBP have been evaluated and the best experimental conditions were chosen is 15 mg of PMBP in 100 mg of MWCNT at 0.1 M PBS (pH 6.4). APAP has a stable current response on PMBP modified CPE where the appeared peak current was well-defined and enhanced greatly compared to bare MWCNT. The modified sensor displays high sensitivity, good selectivity, and a low LOD with APAP.

Acknowledgements

The authors would like to express their gratitude to the Sultan Idris Education University (UPSI) for the Rising Star Grant (Grant Number: 2019-0120-103-01) in funding the research.

References

1. R. Gulaboski and C. M. Pereira, *Electroanalytical Techniques and Instrumentation in Food Analysis. Handbook of Food Analysis Instruments*, CRC Press, London, p. 379 (2008).
2. N. Sharma, V. Mutreja and H. Kaur, Electrochemical Sensors. *Eur. J. Mol. Clin. Med.*, **7**, 4519 (2020).
3. N. R. Stradiotto, H. Yamanaka and M. V. B. Zanoni, Electrochemical Sensors: A Powerful Tool in Analytical Chemistry, *J. Braz. Chem. Soc.*, **14**, 159 (2003).
4. J. Baranwal, B. Barse, G. Gatto, G. Broncova and A. Kumar, Electrochemical sensors and their applications: A review. *Chemosensors*, **10**, 363 (2002).
5. S. Weheabby, Z. Wu, A. Al-Hamry, I. A. Pašti, A. Anurag, D. Dentel, C. Tegenkamp, and O. Kanoun, Paracetamol detection in environmental and pharmaceutical samples using multi-walled carbon nanotubes decorated with silver nanoparticles. *Microchemical Journal*, **193**, 109192 (2023).
6. I. H. Cho, D. H. Kim and S. Park, Electrochemical biosensors: Perspective on functional nanomaterials for on-site analysis. *Biomaterials research*, **24**, 1 (2020).
7. S. Chetana, N. Kumar, P. Choudhary, G. Amulya, C. S. Anandakumar, K. B. Kumar and D. Rangappa, Cu_2ZnSnS_4/MoS_2/CNT-ternary heterostructures for paracetamol determination. *Materials Chemistry and Physics*, **294**, 126869 (2023).
8. Ž. Z. Tasić, M. B. P. Mihajlović, A. T. Simonović, M. B. Radovanović and M. M. Antonijević, Review of Applied Surface Modifications of Pencil Graphite Electrodes for Paracetamol Sensing, *Results Phys*., **22**, 103911 (2021).
9. A. Pollap, K. Baran, N. Kuszewska and J. Kochana, Electrochemical sensing of ciprofloxacin and paracetamol in environmental water using titanium sol based sensor, *J. Electroanal. Chem.*, **878**, 114574 (2020).
10. H. Montaseri and P. B. Forbes, Analytical techniques for the determination of acetaminophen: A review, *TrAC - Trends Anal. Chem*., **108**, 122 (2018).
11. M. Javad Tavakoli, M. Shabani-Nooshabadi, M. and N. Ziaie, Application of Gd_2ZnMnO_6/ZnO nanocomposite for electrochemical measurement of acetaminophen, diphenhydramine, and phenylephrine. *Analytica Chimica Acta*, 341766 (2023).
12. R. Porada, N. Wenninger, C. Bernhart, K. Fendrych, J. Kochana, B. Baś, K. Kalcher, K. and A. Ortner, Targeted modification of the carbon paste electrode by natural zeolite and graphene oxide for the enhanced analysis of paracetamol. *Microchemical Journal*, **187**, 108455 (2023).
13. L. S. Manjunatha, B. K. Swamy and K. G. Manjunatha, Cadmium oxide nanoparticle modified carbon paste electrode sensor for sulfadiazine: A voltammetric study. *Inorganic Chemistry Communications*, **150**, 110534 (2023).
14. G. V. Prasad, V. Vinothkumar, S. J. Jang and T. H. Kim, Multi-walled carbon nanotube/graphene oxide/poly (threonine) composite electrode for boosting electrochemical detection of paracetamol in biological samples. *Microchemical Journal*, **184**, 108205 (2023).
15. M. Ghadirinataj, S. K. Hassaninejad-Darzi and H. Emadi, An electrochemical nanosensor for simultaneous quantification of acetaminophen and acyclovir by ND@ Dy2O3-IL/CPE. *Electrochimica Acta*, **450**, 142274 (2023).

16. M. Gharous, L. Bounab, F. J. Pereira, M. Choukairi, R. López, R. and A. J. Aller, Electrochemical Kinetics and Detection of Paracetamol by Stevensite-Modified Carbon Paste Electrode in Biological Fluids and Pharmaceutical Formulations. *International Journal of Molecular Sciences*, **24**, 11269 (2023).
17. N. Ziaie and M. Shabani-Nooshabadi, Application of the $C–C_3N_4/Li_2CoMn_3O_8$/IL nanocomposite for design a sensitive electrochemical sensor in order to detection of cetirizine, acetaminophen and phenylephrine in biological and pharmaceuticals samples. *Environmental Research*, **216**, 114667 (2023).
18. G. Mustafa, M. Zia-ur-Rehman, S. H. Sumrra, M. Ashfaq, W. Zafar and M. Ashfaq, A Critical Review on Recent Trends on Pharmacological Applications of Pyrazolone Endowed Derivatives, *J. Mol. Struct*., **1262**, 133044 (2022).
19. C. Xu and Y. Qian, The α, β-unsaturated pyrazolone-based fluorescent sensor with red emission and its application for real-time monitoring hypochlorite in cancer cells and zebrafish, *Dyes Pigm*., **161**, 303 (2019).
20. I. Althagafi, N. M. El-Metwaly, M. G. Elghalban, T. A. Farghaly and A. M. Khedr, Synthesis of pyrazolone derivatives and their nanometer Ag(I) complexes and physicochemical, DNA binding, antitumor, and theoretical implementations, *Bioinorg. Chem. Appl.*, 2727619 (2018).
21. Z. Dan and L. Jin-zhou, Acylpyrazolone modified glassy carbon electrode effect on the electrochemical behavior of tyrosine, *Anal. Lett.*, **41**, 2832 (2008).
22. F. Marchetti, C. Pettinari, C. Di Nicola, A. Tombesi and R. Pettinari, Coordination chemistry of pyrazolone-based ligands and applications of their metal complexes, *Coord. Chem. Rev*., **401**, 213069 (2019).
23. L. Xu, N. Li and J. Li, Electrochemical study on adsorptive wave of Tin-PMHP complex. *Int. J. Electrochem. Sci*, **7**, 11558-11563 (2012).
24. H. Han, J. Z. Li and X. Z. Pang, Electrochemical sensor using glassy carbon electrode modified with HPMαFP/PPY/GCE composite film for determination of ofloxacin. *International Journal of Electrochemical Science*, **8**, 9060-9070 (2013).
25. Y. Song, and J. Li, Electrochemical sensor using glassy carbon electrode modified with acylpyrazolone-multiwalled carbon nanotube composite film for determination of xanthine. *Journal of Solid State Electrochemistry*, **16**, 689-695 (2012).
26. X. Li, and J. Li, Direct determination of guanine in aciclovir dispersible tablets solution by acylpyrazolone modified glassy carbon electrode. *Reviews in Analytical Chemistry*, **30**, 23 (2011).
27. Y. Song and J. Z. Li, Direct electrochemical determination of adenine using HPMαFP-modified glassy carbon electrode in commercial pharmaceutical products. *Instrumentation Science and Technology*, **39**, 261 (2011).
28. E. N. M. Mahbob, M. S. Ahmad, I. M. Isa, N. Hashim, A. Ul-Hamid, M. I. Saidin, and S. M. Si, Electrochemical sensor of multiwalled carbon nanotube electrode modified by 1-phenyl-3-methyl-4-orthofluoro benzoyl-5-pyrazolone for sensing dopamine. *Bulletin of the Chemical Society of Ethiopia*, **37**, 845 (2023).
29. H. Sosidi, I. Noviandri, and B. Buchari, Synthesis and characterization of 1-phenyl-3-methyl-4-benzoylpyrazolone-5 (HPMBP) and its application as ionophore in Neodymium (III) selective membrane electrodes. *International Journal of Applied*, ***7*(4)**, (2017).
30. S. Malik, A. Khan, H. Khan, G. Rahman, N. Ali, S. Khan and M. D. P. T. Sotomayor, Biomimetic electrochemical sensors based on core-shell imprinted polymers for targeted sunset yellow estimation in environmental samples. *Biosensors*, **13**, 429 (2023).
31. R. Zainul, N. Abd Azis, I. M. Isa, N. Hashim, M. S. Ahmad, M. I. Saidin and S. Mukdasai, Zinc/aluminium–quinclorac layered nanocomposite modified multi-walled carbon nanotube paste electrode for electrochemical determination of bisphenol A, *Sensors*, **19**, 941 (2019).
32. P. K. Kalambate, B. J. Sanghavi, S. P. Karna and A. K. Srivastava, Simultaneous voltammetric determination of paracetamol and domperidone based on a graphene/platinum nanoparticles/nafion composite modified glassy carbon electrode, *Sens. Actuators B Chem.*, **213**, 285 (2015).
33. P. Knihnicki, A. Skrzypek, M. Jakubowska, R. Porada, A. Rokicińska, P. Kuśtrowski, P. Koscielniak and J. Kochana, Electrochemical sensing of Pb^{2+} and Cd^{2+} ions with the use of electrode modified with carbon-covered halloysite and carbon nanotubes, *Molecules*, **27**, 4608 (2022).
34. X. Wang, M. Li, S. Yang, X. Bai and J. Shan, Self-assembled $Ti_3C_2T_X$ MXene/graphene composite for the electrochemical reduction and detection of *p*-nitrophenol, *Microchem. J*., **179**, 107473 (2022).
35. J. Li, Y. Ma, Z. Ye, M. Zhou, H. Wang, C. Ma, D. Wang, P. Huo and Y. Yan, Fast electron transfer and enhanced visible light photocatalytic activity using multi- dimensional components of carbon quantum dots@ 3D daisy-like In2S3/single-wall

carbon nanotubes, *Appl. Catal. B: Environ*., **204**, 224 (2017).
36. M. S. Ahmad, I. M. Isa, N. Hashim, S. M. Si and M. I. Saidin, A highly sensitive sensor of paracetamol based on zinc-layered hydroxide-*L*-phenylalanate modified multiwalled carbon nanotube paste electrode, *J. Solid State Electrochem*., **22**, 2691 (2018).
37. S. Damiri, H. R. Pouretedal and M. Mahmoudi, Sensitive electrocatalytic assay of cyclotetramethylene tetranitramine (HMX) explosive on carbon nanotube/Ag nanocomposite electrode, *Iran. J. Catal.*, **12**, 69 (2022).
38. R. Zainul, N. Hashim, S. N. A. M. Yazid, S. N. M. Sharif, M. S. Ahmad, M. I. Saidin, M. M. C. Sobry, and I. M. Isa, Magnesium layered hydroxide-3-(4-methoxyphenyl) propionate modified single-walled carbon nanotubes as sensor for simultaneous determination of Bisphenol A and Uric Acid. *International Journal of Electrochemical Science*, **16(9)**, 210941 (2021).
39. K. S. Ngai, W. T. Tan, Z. Zainal, R. Mohd Zawawi and J. C. Juan, Electrocatalytic study of paracetamol at a single-walled carbon nanotube/nickel nanocomposite modified glassy carbon electrode, *Adv. Mater. Sci. Eng*., 742548 (2015).
40. H. Ghadimi, R. M. Tehrani, A. S. M. Ali, N. Mohamed and S. Ab Ghani, Sensitive voltammetric determination of paracetamol by poly(4-vinylpyridine)/multiwalled carbon nanotubes modified glassy carbon electrode, *Anal. Chim. Acta*, **765**, 70 (2013).
41. S. Agrahari, A. K. Singh, R. K. Gautam and I. Tiwari, Voltammetric analysis of epinephrine using glassy carbon electrode modified with nanocomposite prepared from Co-Nd bimetallic nanoparticles, alumina nanoparticles and functionalized multiwalled carbon nanotubes, *Environ. Sci. Pollut. Res*., 1 (2022).
42. M. S. S. Adam and E. F. Newair, Square-wave and cyclic voltammetry of native proanthocyanidins extracted from Grapevine (*Vitis vinifera*) on the glassy carbon electrode, *Chemosensors*, **10**, 429 (2022).
43. P. K. Brahman, L. Suresh, V. Lokesh and S. Nizamuddin, Fabrication of highly sensitive and selective nanocomposite film based on CuNPs/fullerene-C60/MWCNTs: An electrochemical nanosensor for trace recognition of paracetamol, *Anal. Chim. Acta*, **917**, 107 (2016).
44. N. S. Anuar, W. J. Basirun, M. Ladan, M. Shalauddin and M. S. Mehmood, Fabrication of platinum nitrogen-doped graphene nanocomposite modified electrode for the electrochemical detection of acetaminophen, *Sens. Actuators B Chem*., **266**, 375 (2018).
45. T. Kokab, A. Shah, M. A. Khan, M. Arshad, J. Nisar, M. N. Ashiq and M. A. Zia, Simultaneous femtomolar detection of paracetamol, diclofenac, and orphenadrine using a carbon nanotube/zinc oxide nanoparticle-based electrochemical sensor, *ACS Appl. Nano Mater*., **4**, 4699 (2021).
46. S. D. Sukanya, B. E. Swamy, J. K. Shashikumara, S. C. Sharma and S. A. Hariprasad, Poly (Orange CD) sensor for paracetamol in presence of folic acid and dopamine, *Sci. Rep*., **11**, 1 (2021).
47. A. S. Farag, Voltammetric determination of acetaminophen in pharmaceutical preparations and human urine using glassy carbon paste electrode modified with reduced graphene oxide, *Anal. Sci*., **38**, 1213 (2022).
48. Y. Kang, N. Shang, X. Lan, S. Wu, J. Zhao, M. Li and Y. Zhang, Preparation of Pt nanoparticles embedded on ordered mesoporous carbon hybrids for sensitive detection of acetaminophen, *Colloids Surf. A: Physicochem. Eng. Asp.*, **641**, 128620 (2022).
49. M. Kumar, B. K. Swamy, C. Sravanthi, C. P. Kumar and G. K. Jayaprakash, $NiFe_2O_4$ nanoparticle modified electrochemical sensor for the voltammetric study of folic acid and paracetamol, *Mater. Chem. Phys.*, **284**, 126087 (2022).
50. A. U. Alam, Y. Qin, M. M. Howlader, N. X. Hu and M. J. Deen, Electrochemical sensing of acetaminophen using multi-walled carbon nanotube and β- cyclodextrin, *Sens. Actuators B Chem*., **254**, 896 (2018).
51. L. V. da Silva, N. D. dos Santos, A. K. de Almeida, D. D. E. dos Santos, A. C. F. Santos, M. C. França, D. J. P. Lima, P. R. Lima and M. O. Goulart, A new electrochemical sensor based on oxidized capsaicin/multi-walled carbon nanotubes/glassy carbon electrode for the quantification of dopamine, epinephrine, and xanthurenic, ascorbic and uric acids, *J. Electroanal. Chem*., **881**, 114919 (2021).
52. L. Sun, M. Yang, H. Guo, T. Zhang, N. Wu, M. Wang, F. Yang, J. Zhang and W. Yang, COOH-MWCNT connected COF and chemical activated CTF as a novel electrochemical sensing platform for simultaneous detection of acetaminophen and p-aminophenol, *Colloids Surf. A: Physicochem. Eng. Asp*., **647**, 129092 (2022).